arXiv:2009.10085

THE MOSDEF SURVEY: THE FIRST DIRECT MEASUREMENTS OF THE NEBULAR DUST ATTENUATION CURVE AT HIGH REDSHIFT*

NAVEEN A. REDDY[1], ALICE E. SHAPLEY[2], MARISKA KRIEK[3], CHARLES C. STEIDEL[4], IRENE SHIVAEI[5,6], RYAN L. SANDERS[6,7], BAHRAM MOBASHER[1], ALISON L. COIL[8], BRIAN SIANA[1], WILLIAM R. FREEMAN[1], MOJEGAN AZADI[9], TARA FETHEROLF[1], GENE LEUNG[8], SEDONA H. PRICE[10], TOM ZICK[3]

DRAFT: September 23, 2020

Background :近傍銀河のextinction curve (EC)
- Nebular emission : MW (Cardelli+89)
- Stellar continuum : Calzetti00

銀河(hi-zでも)のextinctionはnebular emissionのほうが大きな値
⇒ EC はhi-zではどうなっている？

532 MOSDEF SFG @ z=1.4-2.6
- Composite spectra : Haで規格化
- Stellar continuum + Ha-Heまでの5つの輝線フィット：吸収も考慮できている

Table 2
Samples, Balmer Emission-Line Coverage, and Line Flux Ratios

Sample	N^b	z-Range ($\langle z\rangle$)^c	Hα	Hβ	Hγ	Hδ	Hε^d	Subset of^e
S1	240	1.2467 – 2.6403 (1.9424)	1.000 ± 0.004	0.234 ± 0.004	0.085 ± 0.004	—	—	—
S2	130	1.3631 – 2.6196 (1.5875)	1.000 ± 0.004	0.224 ± 0.004	0.085 ± 0.004	0.038 ± 0.004	—	S1, S7
S3	72	1.5031 – 2.1230 (1.6719)	1.000 ± 0.005	0.225 ± 0.006	0.076 ± 0.006	0.033 ± 0.005	0.020 ± 0.007	S1-S2, S4-S9
S4	355	1.5031 – 2.4225 (2.1041)	1.000 ± 0.003	0.247 ± 0.003	—	—	0.024 ± 0.004	—
S5	80	1.5031 – 2.4225 (1.7433)	1.000 ± 0.005	0.227 ± 0.006	0.077 ± 0.006	—	0.021 ± 0.007	S1, S4
S6	278	1.5031 – 2.3104 (2.0384)	1.000 ± 0.003	0.247 ± 0.003	—	0.044 ± 0.003	0.023 ± 0.004	S4, S9
S7	141	1.3549 – 2.6196 (1.6206)	1.000 ± 0.004	—	0.085 ± 0.004	0.038 ± 0.004	—	—
S8	82	1.5031 – 2.1244 (1.7213)	1.000 ± 0.005	—	0.077 ± 0.006	0.033 ± 0.005	0.019 ± 0.007	S7, S9
S9	289	1.5031 – 2.3104 (2.0401)	1.000 ± 0.003	—	—	0.044 ± 0.003	0.022 ± 0.004	—

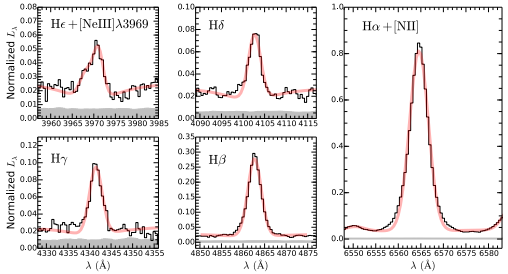

Figure 1. Composite spectrum constructed for sample S4 (Table 2), shown in black, along with fits to each of the Balmer emission lines (red). The error spectrum is indicated in grey. For sample S4, only Hα, Hβ, and Hε were used to compute the attenuation curve (Section 3).

tion curve. The functional forms of $k'(\lambda)$ versus $1/\lambda$ are

$$k'_{\rm L}(\lambda) = -2.479 + \frac{2.286}{\lambda} \quad (7)$$

for the linear-in-$1/\lambda$ fit and

$$k'_{\rm Q}(\lambda) = 2.074 - \frac{2.519}{\lambda} + \frac{1.196}{\lambda^2} \quad (8)$$

for the quadratic-in-$1/\lambda$ fit for $0.38 \lesssim \lambda \lesssim 0.66\,\mu$m. The

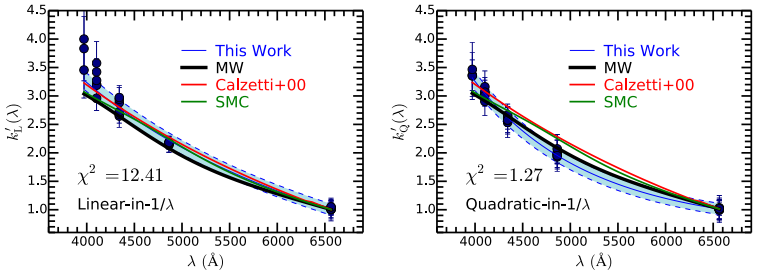

Figure 3. $k'(\lambda)$ versus λ for the linear-in-$1/\lambda$ (*left*) and quadratic-in-$1/\lambda$ polynomial forms (*right*). Measurements are shown by the blue circles—these values differ between the two polynomial forms since $k'(\lambda)$ depends on $E(B-V)_{\rm neb}$, and the latter depends on the functional form used to fit $A'(\lambda)$. Error bars for each $k'(\lambda)$ point are also shown. The best-fit polynomial and 95% confidence intervals are denoted by the solid and dashed blue lines, respectively. The reduced χ^2 for the fits are indicated in each panel. For comparison, the MW extinction curve, shifted so that its value at the wavelength of Hα is equal to that of the curve derived here, is shown by the thick black line. Similarly, the shifted SMC and Calzetti et al. (2000) curves are shown by the solid green and red lines, respectively.

- 誤差の範囲内で近傍のECと一致
- E(B-V)を決めるとき、A(λ)をどうフィットするかで結果が20%くらい違う
- Quadraticのほうがフィットも良いし、より正しいだろう
- より短波長側の情報が欲しいところ
- Rv(L)=3.34 / Rv(Q)=3.09 : これもMWとconsistent

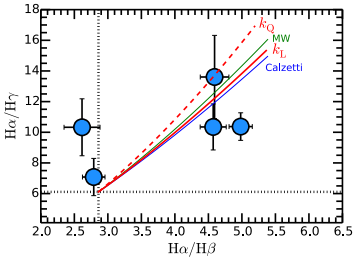

Figure 4. Ratios of Hα/Hγ versus Hα/Hβ for five galaxies where Hα, Hβ, and Hγ are detected with $S/N \geq 5$ (points). The relationships between these ratios for different attenuation curves are indicated by the curves, including the linear and quadratic forms given by Equations 9 and 10, where reddening increases towards the upper right-hand side of the figure. The SMC curve lies very close to that of the Calzetti et al. (2000) curve, and the Reddy et al. (2015) curve lies very close to $k_{\rm L}(\lambda)$, on this figure. The dotted lines indicate the intrinsic line ratios. The two objects whose ratios lie below the intrinsic values are consistent within 3σ of having very little reddening.

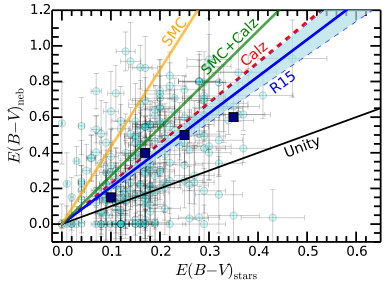

Figure 5. Nebular reddening, derived assuming the $k_{\rm Q}(\lambda)$ parameterization of the nebular attenuation curve, versus the reddening of the stellar continuum for individual galaxies (circles) with the fiducial modeling described in Section 2.4, i.e., assuming the Reddy et al. (2015) (R15) attenuation curve.

$$E(B-V)_{\rm neb} = (2.070 \pm 0.088) \times E(B-V)_{\rm stars}. \quad (12)$$

E(B-V)nebとE(B-V)starsの違いの原因は？
1. 生まれた星のmolecular cloud (MC) crossing time (1-3Myr)がBalmer emissionのメインとなる >O6星の年齢より長いため
   - ただし、Binaryがhi-zで卓越する仮説を採用すると、大質量星の寿命が数倍のびる => MC crossing timeも数倍長くなる (そうするとMCの分裂タイムスケールに近くになる?)
2. あるいは rising star formation history のせい？
   - ダスト吸収の少ない古い星形成+ダスト吸収が強い若い星形成
3. あるいはダストが星間空間により広く広がっている？どういうことか？